Analysis of the Near-Infrared Spectral Characteristics of Dairy Farm Slurry under Temperature Variations Using Two-Dimensional Correlation Spectroscopy

Peng Wang[a#], Junjie Che[b#], Cheryl Marie Cordeiro[c], Shengbo Liu[a, d], Ben Aernouts[e], Mengting Li[a], Erik Sindhøj[f], Haibo Ma[g], Heinz W. Siesler[h], Keqiang Zhang[a], Zengjun Yang[a *], Run Zhao[a *]

[a] *Agro-Environmental Protection Institute, Ministry of Agriculture and Rural Affairs, 31 Fukang Road, Tianjin, China*

[b] *Yichun Science and Technology Information Institute, Yichun, China*

[c] *Division of Urban Development, RISE Research Institutes of Sweden, Sven Hultin Plats 5 (Headquarters), Gothenburg, Sweden*

[d] *College of Resources and Environment, Northeast Agricultural University, Harbin, China*

[e] *Department of Biosystems, Animal and Human Health Engineering Unit, Geel campus, KU Leuven, Kleinhoefstraat 4, 2440 Geel, Belgium*

[f] *Division of Bioeconomy, RISE Research Institutes of Sweden, Ultunaallén 4, Uppsala, Sweden*

[g] *Tianjin Jialihe Livestock Group Co., Ltd.*

[h] *Department of Physical Chemistry, University Duisburg-Essen, Schuetzenbahn 70 Essen, Germany*

[#] The first two authors contributed equally to this manuscript.

*The corresponding author at

Corresponding author: yangzengjun@caas.cn, zhaorun01@caas.cn

Abstract: Near-infrared spectroscopy (NIRS) is a powerful tool for the rapid identification and quantitative analysis of dairy farm slurry components. Temperature variations significantly influence on the spectra measurements while their underlying spectral response mechanisms remain insufficiently understood. This study investigates the impact of temperature variations on the spectral characteristics of slurry to ascertain the availability of improving the NIRS-based analysis. Using a portable detection device of slurry nutrients, near-infrared diffuse reflectance spectra were acquired from slurry samples across temperatures ranging from 0 to 40°C. Principal component analysis (PCA) and two-dimensional correlation spectroscopy (2D-COS) were applied

to assess spectral response intensity, temporal sequence and correlations among functional groups. The results indicate that increasing temperature weakens hydrogen bonding strength, leading to intensity changes and shifts of specific absorption bands. Notably, hydrogen-bonded water molecules are observed to dissociate, leading to an increase in spectral features associated with free O-H groups, which strongly suggests temperature-induced changes in intermolecular interactions. Additionally, elevated temperatures increase the susceptibility of specific absorption bands (ν(N-H), and ν(O-H)) to shift, affecting the stability of slurry composition predictions. 2D-COS analysis reveals the sequential evolution of absorption band changes of specific functional groups under thermal effects, providing insights into their dynamic transformations. While 2D-COS has been previously applied to various agricultural materials, this study extends its application to temperature-induced spectral analysis of dairy farm slurry, addressing a specific challenge in NIRS-based nutrient analysis where conventional temperature correction approaches have shown limitations. By identifying temperature-sensitive spectral regions and molecular transformations, this study provides a scientific basis for developing temperature-resilient NIRS models, which are crucial for facilitating real-time nutrient monitoring and precision slurry management on dairy farms.

Keywords: dairy farm slurry, temperature effects, near-infrared spectroscopic analysis, two-dimensional correlation spectroscopy, hydrogen bonding.

1 Introduction

With the rapid intensification of dairy farming, effective slurry management is essential for environmental sustainability and agricultural productivity [1]. Dairy slurry is a nutrient-rich mixture of feces, urine, bedding material, and parlour washings, containing essential elements such as nitrogen (N) and phosphorus (P). It serves as a valuable resource for fertilization, but its high variability and complex composition pose significant challenges for accurate nutrient quantification, hindering precision slurry application and efficient resource utilization [2].

Near-Infrared Spectroscopy (NIRS) is a widely recognized technique for rapid, non-invasive and simultaneous analysis of slurry multi-composition [3]. Studies have successfully applied NIRS to quantify key slurry components, including N, P, potassium, and organic matter [4,5]. However, a significant limitation remains: NIRS measurements are sensitive to external factors, especially temperature fluctuations, due to the strong dependence of water absorption on temperature in the near-infrared region [6,7]. Temperature fluctuations alter hydrogen bonding interactions, leading to shifts of absorption bands and measurement errors exceeding 40% in some cases [8,9].

Existing temperature correction models attempt to compensate for these errors but face several limitations. Many rely on empirical regression models that fail to capture the nonlinear effects of temperature on slurry composition [10]. Others employ standardization techniques that assume uniform spectral responses across different slurry samples, which do not account for compositional variability or interactions between functional groups [11]. The overlapping absorption bands in the NIR spectra of slurry spectra further complicate correction efforts, making it difficult to distinguish temperature-induced spectral distortions from genuine compositional changes [12]. Thus, this remains a critical gap in developing a systematic, high-resolution approach to understanding and correcting temperature-dependent spectral variations in slurry.

To address the defect, two-dimensional correlation spectroscopy (2D-COS) has been introduced with wide applications across many systems, including controlled solutions (ethylene glycol solutions, chemical interactions, polycyclic aromatic hydrocarbons) and agricultural materials such as manure-derived biochar and digestate [13-16]. A key advantage of 2D-COS is its capability to resolve the sequence of spectral changes induced by a specific perturbation. In this study, by applying thermal perturbation to slurry samples from a specific treatment stage where compositional variability is minimized, 2D-COS was employed to isolate the sequential response of functional groups to temperature changes from the spectral compositional background. This approach helps in identifying temperature-sensitive spectral regions [17]. This capability makes it particularly promising for addressing temperature interference in

dairy slurry NIRS analysis, where conventional spectral correction techniques have shown limitations.

In this study, we combined the use of portable instruments for on-site sampling and testing, and simulated field temperature variation in the laboratory, to explore the spectral response characteristics and interference mechanism. Although temperature effects on livestock slurry NIRS have been extensively documented using traditional spectroscopic approaches [6,12], the application of 2D-COS specifically to probe temperature-induced NIR spectral changes in dairy slurry has not to our knowledge, been previously reported. The present study addresses this gap by applying 2D-COS to dairy slurry NIR spectra to investigate how temperature disturbances influence spectral characteristics and molecular transformations. Using abundant slurry samples from a commercial dairy farm in Tianjin, we integrate Principal Component Analysis (PCA), baseline correction, and 2D-COS to identify characteristic spectral responses under temperature fluctuations, elucidate temperature-induced molecular transformations in hydrogen bonding networks, to provide the basis for improving temperature correction strategy. This approach extends the application domain of 2D-COS from previous agricultural studies to the specific challenge of scene temperature correction in dairy slurry NIRS, contributing to more reliable, real-time nutrient assessment for precision slurry management.

2 Materials and Methods

2.1 Collection of Slurry Samples and Selection of Sampling Sites

A commercial-scale dairy farm located in eastern Tianjin's Ninghe District was selected as the case study location for this research. The farm maintains a herd of approximately 2700 cattle, including 1400 adult milking cows and 920 heifers, and manages about 67 hectares of arable land for slurry recycling.

The manure management system consists of collection, transport and treatment stages, covering solid-liquid separation, homogenization and regulation, anaerobic fermentation, sedimentation, and storage in tanks and lagoons prior to land application. Manure is regularly scraped to the gutters inside the end of barns, then washed away to the solid-liquid separation unit (collection tank, stirring paddle, separator and

separation tank) via underground pipelines. Separated slurry from heifer separation tank was conveyed to the mixed collection tank. Parts of wastewater from the milking unit was also pumped to the mixed collection tank to adjust the solid-liquid ratio. After separation, the liquid phase (hereafter referred to as slurry) flows into the regulation tank, which functions as a mixing and equalization stage, regulate feeding the anaerobic digester. After anaerobic fermentation, the digestate is directed to a sedimentation tank before being pumped to the storage lagoon.

Three sampling campaigns were conducted from April to June 2022, covering all major stages of the slurry-handling chain. Multiple slurry samples were collected from nine sites ranging from the manure gutters of different barns, collection and separation tanks, regulation tank, sedimentation tank and storage lagoons. In total, 320 slurry samples were collected. To maintain sample integrity, the samples were transported in insulated containers with ice packs and transferred to the laboratory for timely testing.

Li et al. [8] previously demonstrated that the chemical composition of dairy slurry changes markedly across these four main stages (manure gutter, regulating tank, sedimentation tank and lagoon) of the handling chain, reflecting microbial transformations before and after anaerobic fermentation. These stages were therefore chosen for the present analysis to capture representative compositional and spectral variability throughout the handling process.

2.2 Temperature Gradient Setup and Spectroscopic Data Collection

The temperature range was designed based on the local ambient temperature in Ninghe District, during the sample collection period (April to June 2022). Sample temperature regulation and measurement were conducted using a Shanghai Shuoguang AI 1511 C series compact portable metal bath (precision: ±0.3°C) and a high-precision digital thermometer from Hengshui Zhengxu Co., Ltd. (precision: ±0.1°C). Spectra were collected sequentially from 0 °C to 40 °C in 5 °C increments (9 temperature levels). At each temperature, samples were equilibrated for 15 min to ensure uniform temperature before scanning. The sequential order was chosen to avoid condensation when handling colder samples and to ensure stable equilibration at each temperature step. To minimize instrumental drift, we used the integrating sphere's built-in reference

for background and each sample was scanned 10 times and the average spectrum obtained as the final spectrum, while temperatures were verified immediately before and after each acquisition ($\Delta T \leq 1$ °C) Sample homogeneity was maintained by gentle stirring immediately before spectral acquisition.

Measurements were performed using a self-integrated On-site Slurry Nutrients Inspection Kit comprising an Ocean Optics NIR Quest 512-1.7 near-infrared spectrometer, an HL-2000 tungsten halogen light source, an InGaAs detector, and an ISP-REF integrating sphere assembly, with a spectral resolution of 3.0 nm. Near-infrared diffuse reflectance spectra were acquired in the wavelength range of 897-1712 nm. In total, 9×320 near-infrared spectra were collected across all temperature levels.

2.3 Data Analysis and Processing

Due to the high dimensionality and overlapping features in the spectral data, PCA was first applied for dimensionality reduction. This process extracted key spectral features and explained data variance, enabling an intuitive understanding of the spectral correlations and distribution patterns at different temperatures. To minimize the effects of baseline drift and other external interferences introduced by temperature variations, baseline correction was applied [18, 19] to remove offset and scattering effects caused by instrument drift. The spectra after baseline correction are called "corrected spectra". Subsequently, 2D-COS was used to analyze the corrected spectra, resolving overlapping absorption bands and revealing the relative directions of intensity changes and sequence information of molecular structural changes. This approach provided deeper insights into the chemical properties of the samples.

2D-COS analysis was restricted to the 897-1712 nm region containing the identified temperature-sensitive peaks. Temperature perturbation was encoded as a linear sequence (0, 5, 10, 15, 20, 25, 30, 35, 40°C) for 2D-COS analysis, with each temperature treated as an equally-spaced perturbation step to ensure proper correlation weighting.

All data processing was conducted in MATLAB, with 2D-COS analysis performed using the 2D-shige software (Prof. Shigeaki Morita, Osaka) and data visualization was carried out in Origin.

3 Results and Discussion

3.1 Principal Component Analysis of Slurry Near-Infrared Spectra Across Various Temperatures

PCA was performed on the 2880 collected slurry spectra to identify correlations and characteristic differences among samples in relation to temperature. The first two principal components (PC1 and PC2) accounted for 99.2% of the total variance, effectively capturing nearly all spectral information. Fig. 1 illustrates the distribution of all spectra in the PC1-PC2 subspace, where distinct temperature-dependent clustering was observed.

In the PC1-PC2 subspace, the PCA score plot shows a clear temperature-dependent pattern. The sequential distribution of sample scores along the first principal component (PC1) (Fig. 1) directly correlates with the temperature gradient. The PC1 values of the 0°C samples are all greater than 0, positioned at the far right of the plot. The PC1 values of the 20°C samples are located in the center around 0, located in the center, while the 40°C samples have PC1 values less than 0, appearing at the far left of the plot. The spectral scores at 0°C show a greater dispersion compared to the tighter clusters observed at higher temperatures, such as 35°C and 40°C. Potential factors may be the challenge of achieving a perfectly uniform equilibrium for the complex slurry matrix at the 0°C.

As temperature increases, the sample scores progressively shift leftward, indicating a systematic spectral response to temperature variations. This leftward shift represents molecular transformations influenced by rising temperature. In practical terms, this means that as the temperature increases, absorption bands - particularly of water specific O-H bonds - shift in a predictable manner. These changes reflect the weakening of hydrogen bonds and increased molecular motion, which must be accounted for in NIRS-based nutrient predictions to avoid misinterpretation of slurry composition. The principal component score plot further reveals a “layering” effect among slurry spectra at different temperatures, confirming that temperature influences the near-infrared diffuse reflectance spectra. If not taken into account when developing a predictive model, this effect can lead to significant inaccuracies in NIRS-based prediction of

nutrient concentrations. A model calibrated on spectra collected at 20°C, for instance, could systematically underestimate or overestimate values when applied to spectra from samples at 0°C or 40°C, respectively. These results underscore the need to account for temperature effects in spectral analysis and highlight the importance of correction models to improve the reliability of NIRS-based slurry assessments.

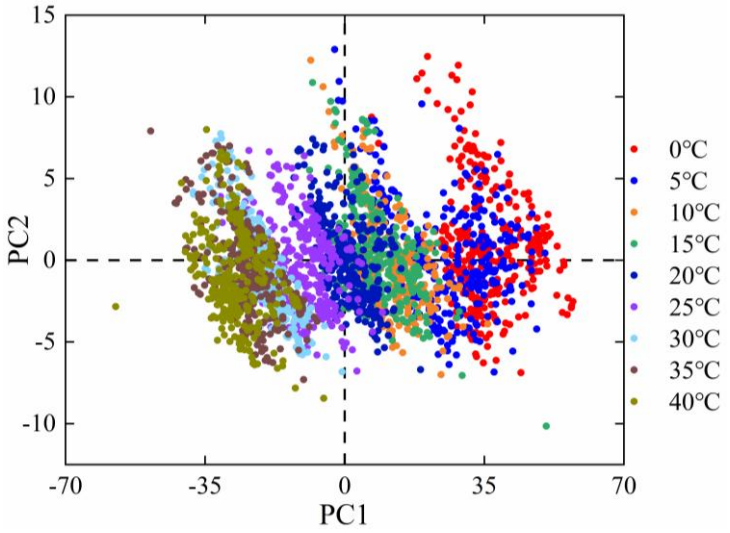


Fig. 1 2D-PCA score plot of the principal components PC1(97.42%) / PC2(1.78%) of the NIR spectra of slurry samples measured at different temperatures.

3.2 Interpretation Near-Infrared Spectra of Slurry in Response to Temperature Perturbations

The original spectra and corrected spectra of samples collected from the four locations (manure gutter, regulating tank, sedimentation tank and lagoon) at different temperatures (Fig. 2) exhibit five distinct spectral peaks. These peaks are observed within the following wavelength ranges: 934-998 nm, 1132-1245 nm, 1312-1365 nm, 1379-1429 nm, 1467-1578 nm. These peaks can be tentatively attributed to the 2nd overtone of ν(O-H)$_{free}$ stretching vibration, a combination band of ν(O-H)$_{ass}$ + first overtone of ν(C-H) stretching vibrations, combination bands of the first overtone of ν(C-H) stretching + δ(CH$_2$) deformation vibrations, and the first overtone of the ν(N-H) stretching vibration, respectively[20, 21]. However, it is crucial to note that in a water-rich system like slurry, these spectral regions are also highly sensitive to the reorganization of the water hydrogen-bonding network. Because water absorbance bands overlap with N-H and C-H vibration regions, these assignments should be

considered indicative rather than definitive. As temperature increases, the intensities of the five absorption bands change and shift, consistent with a concomitant weakening of hydrogen bonds involving N-H, and O-H groups. These bonds progressively shift to weaker hydrogen bonds and eventually dissociate into free functional groups. Additionally, since the slurry is predominantly composed of water, which acts as the main absorber, the reduction in hydrogen bonding between water molecules leads to an increase in free molecules.

Both the original and corrected spectra clearly reveal significant differences in spectral profiles between samples collected before anaerobic fermentation (manure gutter and regulating tank) and after anaerobic fermentation (sedimentation tank and lagoon). Notably, the absorption peak within the 1587-1653 nm range disappears after fermentation, suggesting that the slurry composition and nutrient proportions remain relatively unchanged from the manure gutter to the regulating pond, before anaerobic fermentation, and from the sedimentation tank to the lagoon after anaerobic fermentation. However, a direct comparison of spectra before and after fermentation clearly shows spectral shifts, substantial changes in peak intensities, and the disappearance of certain peaks. This indicates pronounced alterations in the slurry's composition and characteristics due to biochemical transformation during anaerobic fermentation. During initiation of anaerobic digestion, the slurry undergoes a series of microbial-driven reactions, including hydrolysis and acidification, leading to the breakdown of large organic molecules into volatile fatty acids (VFAs). These VFAs are subsequently converted into CH_4 and CO_2 by methanogenic bacteria groups, and other bacteria groups lead to a breakdown into NH_3 and H_2S [22-25]. This transformation significantly alters the material composition of the slurry system after anaerobic fermentation.

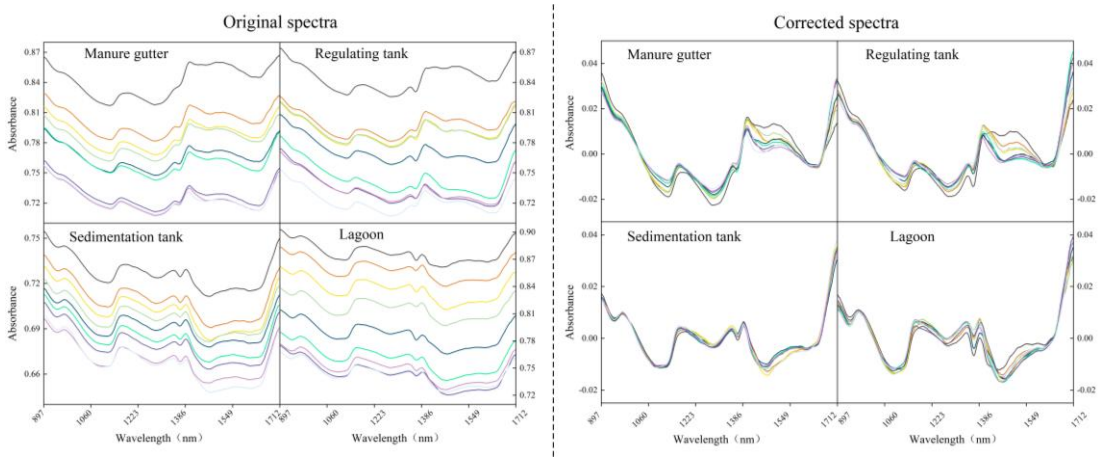


Fig. 2 The original and corrected spectra of samples collected from the four locations (manure gutter, regulating tank, sedimentation tank and lagoon) at different temperatures

3.3 2D-COS Analysis of Slurry Spectra from Typical Sites

Fig. 3 presents the auto-correlation spectra of samples from the four sampling points. The spectra of manure gutter and regulating tank exhibit similar positions of auto-peaks, cross-peaks, and auto-correlation peaks. A comparable pattern is observed in the spectra of the sedimentation tank and lagoon, reinforcing the conclusions drawn from the analysis in section 3.2. Additionally, the auto-correlation spectra of manure gutter and lagoon each exhibit seven temperature-sensitive auto-peaks. Compared to conventional near-infrared spectroscopy, this approach enhances spectral signal detection. Table 1 provides a label of each peak along with the corresponding assignment to functional groups[20, 26]. Based on the corrected spectra and auto-correlation spectral analysis, the manure gutter and lagoon in the slurry treatment chain are identified as representative positions for subsequent analysis.

To clarify the practical significance of these results, the 2D-COS maps illustrate how different molecular bonds respond sequentially to temperature fluctuations. The determination of the transformation sequence is crucial for temperature correction models as it suggests that temperature-induced changes occur in a predictable order. Unlike previous applications of 2D-COS in homogeneous systems, this study applies it to dairy slurry, an extremely complex mixture with significant compositional variability. Our findings extend some previous research results by applying 2D-COS to

heterogeneous biological systems [14, 27], showing that despite the compositional complexity of dairy slurry, molecular transformations due to temperature follow an ordered sequence. Furthermore, this study identifies sequential molecular transformations that were previously unaccounted for in standard NIRS calibration models. By identifying the sequence of spectral shifts, we provide a framework for reducing temperature-related errors in NIRS-based slurry analysis. These results emphasize the need for temperature correction techniques tailored to heterogeneous biological matrices, improving the reliability of rapid nutrient quantification methods. This provides a theoretical basis for a more robust spectral correction model for real-time slurry analysis based on near-infrared spectroscopy.

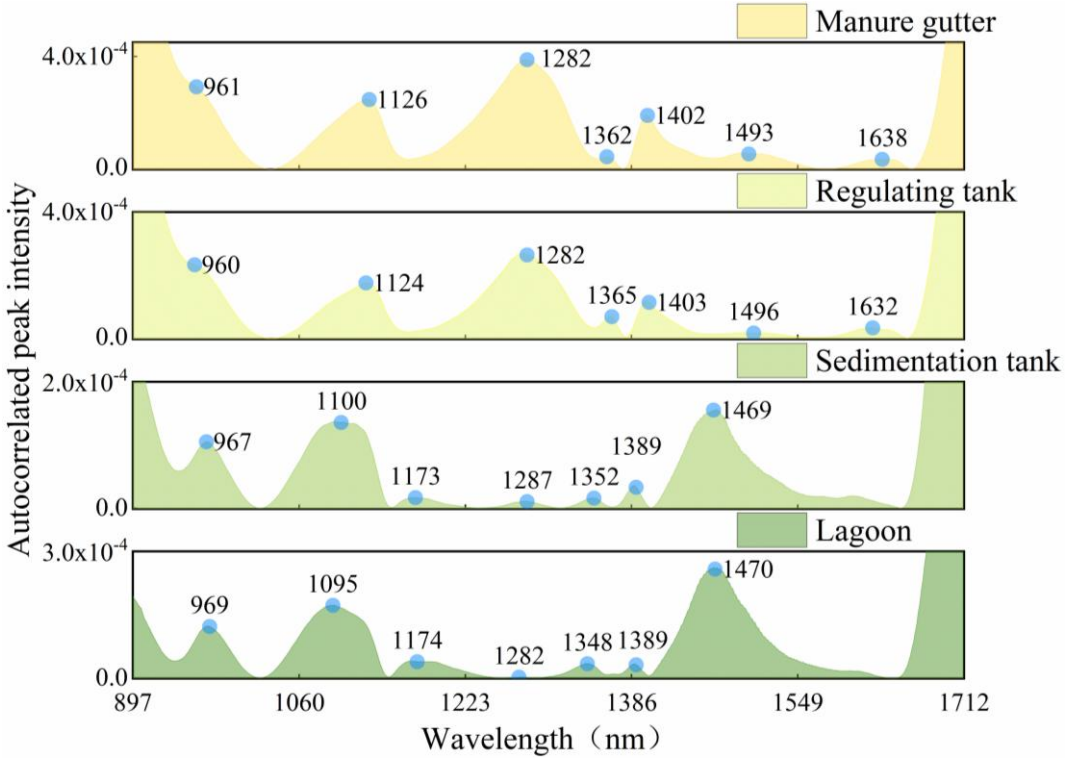


Fig. 3 The autocorrelation spectra of the slurry samples in the wavelength range 897-1712 nm.

Table 1 Wavelength positions and functional group assignments of each peak in the autocorrelation spectrum of the slurry

Site	Label	Characteristic peak(nm)	Functional group	Vibration type
Manure gutter	Mg1	961	Free O-H	2nd Overtone 3v(OH)

	Mg2	1126	Associated O-H, C-H (CH_2)	Combination band v(OH) + 2v(CH)
	Mg3	1282	Free O-H, C-H (CH_2）	Combination band v(OH) + v(CH)+δ(CH_2)
	Mg4	1362	C-H (CH_3, CH_2)	Combination band 2v(CH) + δ(CH_2)
	Mg5	1402	Free O-H	1st Overtone 2v(OH)
	Mg6	1493	Free N-H	1st Overtone 2v(NH)
	Mg7	1638	$(C-H)_{ar}$	1st Overtone 2v$(CH)_{ar}$
Lagoon	L1	969	Free O-H	2nd Overtone 3v(OH)
	L2	1095	Free O-H C-H (CH_2)	Combination band v(OH) + 2v(CH)
	L3	1174	C-H (CH_3, CH_2)	2nd Overtone 3v(CH)
	L4	1282	Free O-H, C-H (CH_2)	Combination band v(OH) + v(CH)+δ(CH_2)
	L5	1348	CH_3-CO-O- (CH_3)	Combination band 2v(CH_3) + δ(CH_3)
	L6	1389	C-H (CH_3, CH_2)	Combination band 2v(CH) + δ(CH_2)
	L7	1470	Free N-H	1st Overtone 2v(NH)

3.3.1 Analysis of Manure gutter Samples Using 2D-COS

Fig. 4(a) and (b) shows the synchronous and asynchronous spectra of the manure gutter samples, while Table 2 lists their cross-peaks. As shown in Fig. 4(a) and the synchronous spectrum in Table 2: Φ(1362,1282) > 0 and Φ(1362,1126) > 0 indicated that the functional groups corresponding to aliphatic C-H bonds (at 1362 nm, 1282 nm, and 1126 nm) changed in the same direction. This meant that these aliphatic chains exhibited cooperative motion during the heating process. Φ(1362,1638) > 0 indicated that the changes in aliphatic C-H bonds and aromatic C-H bonds were also synchronous, suggesting that despite the different affiliations of the chemical bonds (aliphatic and aromatic), they may be similarly affected under thermal perturbation.

Φ(1402,961) > 0 indicated that the two free O-H functional groups changed synchronously. This reinforced the view that the behavior of free O-H groups was

consistent. Meanwhile, $\Phi(1402,1493) > 0$ and $\Phi(961,1493) > 0$ showed that the changes in free O-H and free N-H were in the same direction. This suggested that in the stage of heating, free water molecules and substances containing N-H groups were simultaneously affected by the thermal effect. For instance, the increase in temperature might concurrently promote the intensification of their molecular motion.

$\Phi(1402,1282) < 0$ and $\Phi(1402,1126) < 0$ indicated that the free O-H changed in the opposite direction to the functional groups at 1282 nm and 1126 nm (both containing C-H). This revealed that there might be differences in the temperature response of chemical bonds in different phases or microenvironments within the system. For example, the behavior of free water O-H bonds and the C-H bonds tightly bound to organic matter (particularly the C-H associated with bound O-H at 1126 nm) separated during the heating process.

Following Noda's principles for the order of spectral peak responses [28], the sequential changes in spectral peaks with increasing temperature were observed. The Peak Mg6 changes first, Peaks Mg1, Mg2, Mg3, Mg4, and Mg5 all responded before Peak Mg7. Additionally, Peaks Mg2, Mg3, and Mg4 changed before Peak Mg1, while Peak Mg2 changed before Peak Mg3. Furthermore, Peak Mg2 exhibited delayed responses compared to Peak Mg5, and Peaks Mg1 and Mg4 lagged behind Peak Mg3. The change in Peak Mg1 also followed those of Peak Mg4. As temperature increased in the manure gutter samples, the sequential spectral peak variations were as follows: the 2v of free N-H (1493 nm) > the 2v of free O-H (1402 nm) > the v(OH) + 2v(CH) of associated O-H and C-H (CH_2) (1126 nm) > the v(OH) + v(CH) + δ(CH_2) of free O-H and C-H (CH_2) (1282 nm) > the 2v(CH) + δ(CH_2) of C-H (CH_3, CH_2) (1362 nm) > the 3v of free O-H (961 nm) > the 2v of aromatic C-H (1638 nm). This result aligns with the findings of Ouyang et al. [29], who reported that an increasing temperature disrupts hydrogen bonding and weakens intermolecular forces. The preferential variation of peak Mg6 (2v of free N-H) seen in our study was consistent with their observations.

3.3.2 Analysis of Lagoon Samples Using 2D-COS

Fig. 4(c) and (d) shows the synchronous and asynchronous spectra of the lagoon samples. As shown in Fig. 4(c) and the synchronous spectrum in Table 2, Φ(1348, 1389) > 0, Φ(1348, 1174) > 0, and Φ(1348, 969) > 0 indicated that the variation trend of the C-H bond in the acetyl group (1348 nm) was consistent with that of the C-H bonds in hydrocarbons (1174 nm and 1389 nm) and the free O-H bond (969 nm). This suggested that the methyl vibration of the acetyl group synchronized with the behavior of hydrocarbons and free water in response to temperature changes. Φ(1470, 1348) < 0, Φ(1470, 1174) < 0, and Φ(1470, 969) < 0 indicated that the change in the N-H bond was opposite to the trends of the acetyl C-H bond (1348 nm), the hydrocarbon C-H bond (1174 nm), and the free O-H bond (969 nm). This implied that the behavior of the N-H group was independent of specific hydrocarbons and free water in the system.

Φ(969, 1348) > 0, Φ(969, 1174) > 0, and Φ(969, 1389) > 0 indicated that free water changed synchronously with various C-H bonds. In contrast, Φ(969, 1095) < 0 suggested that the change in free water was opposite to that of Peak L2, which involves combined O-H and C-H vibrations. Φ(1095, 1282) > 0 indicated that Peaks L2 and L4 (both involving free O-H and C-H vibrations) varied synchronously. However, Φ(1095, 969) < 0, Φ(1095, 1174) < 0, Φ(1095, 1348) < 0, and Φ(1095, 1389) < 0 suggested that the functional groups represented by Peak L2 exhibited a distinct behavior in response to temperature changes compared to simple free water or hydrocarbon chains. Φ(1174, 1389) > 0 indicated that the vibrations of methyl and methylene groups in the hydrocarbon chain responded consistently to temperature variations, allowing them to be considered as a whole when examining their interactions with other functional groups.

Following Noda's principles for the order of spectral peak responses. The Peak L7 changes first, the change in Peak L2 precede the changes in Peaks L5, and L6. Additionally, the Peak L5 lag behind on Peaks L1 and L6, while Peak L1 changes after Peak L6. Consequently, the order of spectral peak variations in the lagoon samples with increasing temperature were as follows: 2v of free N-H (1470 nm) > v(OH) + 2v(CH) of free O-H and C-H (CH_2) (1095 nm) > 2v(CH) + δ(CH_2) of C-H (CH_3, CH_2) (1389 nm) > 3v of free O-H (969 nm) > 2v(CH_3) + δ(CH_3) of CH3-CO-O- (CH_3) (1348 nm).

This sequence differs slightly from that observed in manure gutter samples, which may be due to compositional changes before and after anaerobic fermentation. Variations in proportion of each component likely contribute to the observed differences in peak order under temperature disturbances.

Our findings are also supported by previous studies. Bromberg et al. [30] experimentally demonstrated that temperature has a minor effect on hydrocarbon C-H bonds, which is consistent with our result that Peak L5 has a lower priority in spectral changes. Watanabe et al. [31] highlighted the strong influence of temperature on O-H bonds, noting that these bonds were more likely to break at high temperatures. This was consistent with the changed order of Peaks L2 (3v of combined O-H) in this study.

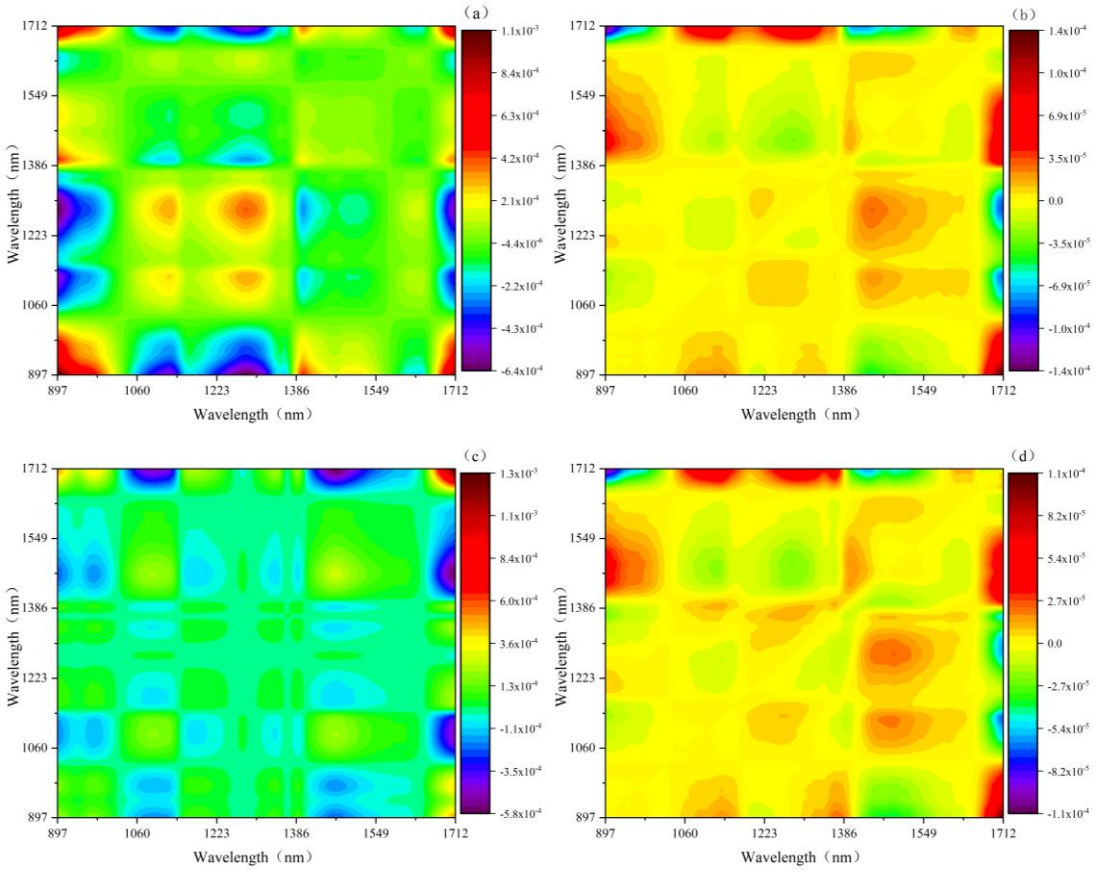


Fig. 4 Synchronous(a) and asynchronous(b) of the manure gutter spectra and synchronous (c) and asynchronous (d) of the lagoon spectra

Table 2 Signs of cross-peaks (synchronous outside parentheses, asynchronous inside parentheses) in the 2D-COS maps of manure gutter and lagoon samples with increasing temperature

	Characteristic peak (nm)	961	1126	1282	1362	1402	1493	1638
Manure gutter	961	+(+)	-(-)	-(-)	-(-)	+(+)	+(+)	-(+)
	1126	-(+)	+(+)	+(-)	+(-)	-(-)	-(-)	+(-)
	1282	-(+)	+(+)	+(-)	+(-)	-(-)	-(-)	+(-)
	1362	-(+)	+(+)	+(+)	+(-)	-(-)	-(-)	+(-)
	1402	+(-)	-(+)	-(+)	-(+)	+(+)	+(+)	-(+)
	1493	+(-)	-(+)	-(+)	-(+)	+(-)	+(+)	-(+)
	1638	-(-)	+(+)	+(+)	+(+)	-(-)	-(-)	+(+)

	Characteristic peak (nm)	969	1095	1174	1282	1348	1389	1470
Lagoon	969	+(-)	-(-)	+(-)	-(-)	+(-)	+(+)	-(-)
	1095	-(+)	+(-)	-(+)	+(-)	-(+)	-(+)	+(+)
	1174	+(+)	-(-)	+(-)	-(-)	+(+)	+(+)	-(-)
	1282	-(+)	+(+)	-(+)	+(-)	-(+)	-(-)	+(-)
	1348	+(+)	-(-)	+(-)	-(-)	+(+)	+(+)	-(-)
	1389	+(-)	-(-)	+(-)	-(+)	+(-)	+(-)	-(-)
	1470	-(+)	+(-)	-(+)	+(+)	-(+)	-(+)	+(+)

3.3.3 Interpretation of Synchronous and Asynchronous 2D-COS Spectra in Temperature-Induced Spectral Shifts

The application of two-dimensional correlation spectroscopy (2D-COS) provides key insights into the sequential molecular transformations occurring under temperature fluctuations. The synchronous spectra reveal simultaneous changes in spectral intensities, whereas the asynchronous spectra indicate a stepwise order of structural modifications among functional groups [28].

In the synchronous spectra, positive cross-peaks between characteristic functional groups suggest that they undergo simultaneous spectral changes, indicating common temperature-dependent structural modifications. For example, the synchronous correlation between bound O-H (1126 nm) and C-H (1282 nm and 1362nm) peaks suggests that both functional groups respond in a coordinated manner to temperature increases, reflecting the disruption of hydrogen bonding networks.

Conversely, asynchronous peaks provide additional temporal information, allowing us to determine the relative order of spectral shifts. The asynchronous cross-peak relationships [Φ (969,1348)>0], [Ψ (969,1348)>0], [Φ (1095,1389)<0], [Ψ (1095,1389)<0], [Φ (1402,1282)<0], [Ψ (1402,1282)<0] suggest that changes in free O-H vibrations precede those in hydrocarbon C-H bonds. This finding is consistent with prior research showing that hydrogen-bonded O-H groups exhibit greater sensitivity to thermal perturbations than C-H groups [32].

However, in the water-dominated system of slurry, spectral analysis faces unique challenges. Due to the dominant absorption of water in the near-infrared first harmonic region, temperature-induced spectral changes may reflect both compositional changes and the recombination of the water matrix itself. Therefore, spectral changes may be attributed to the combined influence of water and components in the slurry. By combining 2D-COS analysis with the framework of water spectroscopy, this study provides a clearer explanation of the nature of temperature-sensitive changes in milk slurry: hydrogen bonding dynamics are the dominant factor, but the fundamental role of water matrix recombination needs to be recognized. This finding underscores that in NIRS-based slurry analysis, temperature correction models need to simultaneously consider the interactions between components and the water environment [14, 33].

Furthermore, following the aquaphotomics perspective [34], water acts as a dominant ‘mirror’ reflecting the molecular dynamics of the entire system. The temperature-induced spectral variations observed in this study, particularly in the O-H combination band regions, are likely a combined effect of both the direct breakdown of hydrogen bonds in water matrix and the indirect influence of temperature on the solute-water interactions. The works by Tan et al. [35] and Kondo et al. [36] demonstrate that deconvoluting these contributions is challenging, and our assignments for specific organic functional groups should be interpreted with this complexity in mind.

3.4 Discussion

The increasing need for rapid, on-site monitoring of slurry composition using portable Near-Infrared Spectroscopy (NIRS) instruments need to address significant challenge in the meantime. Spectral measurements are highly susceptible to varying

environmental conditions, particularly temperature. This study bridges the gap between field application and laboratory-based mechanistic understanding. It employs portable instrumentation for initial field sampling and conducts controlled laboratory simulations to replicate field-encountered problems, with a core focus on exploring the underlying mechanisms of temperature-induced spectral variation.

3.4.1 Analysis of the Temperature Dependence of Slurry

The autocorrelation spectrum serves as a valuable tool for assessing the intensity and distribution of spectral changes under external perturbations, such as temperature fluctuations. In this study, the autocorrelation spectra reveal significant spectral sensitivity to temperature disturbances, highlighting the extent to which near-infrared spectral variations occur in response to changes in slurry temperature [17, 37]. By comparing the autocorrelation spectra and corrected spectra from the manure gutter and lagoon, we identified specific temperature-sensitive absorption peaks, as well as regions in the spectra that remain relatively stable despite temperature variations.

These results provide critical insights into the temperature dependence of key chemical bonds in slurry, particularly those involving hydrogen bonding (O-H, N-H) and hydrocarbon interactions (C-H). As temperature increases, weaker hydrogen bonds break, leading to spectral shifts that complicate NIRS-based composition analysis.

3.4.2 Spectral Peak Shifts and Compositional Differences Across Treatment Stages

The most temperature-sensitive spectral peaks were observed at 1282 nm and 1126 nm in manure gutter samples, and 1470 nm, 1095 nm, and 969 nm in lagoon samples. This difference is mainly attributed to the differences between the two treatment approaches, which in turn affects the chemical composition, physical state, and microbial activity. Specifically, the samples from the manure gutter are relatively fresh. Since the samples in the manure gutter stay for a short time, limiting substantial decomposition, they still contain a great deal of hydrocarbons, which exhibit C-H stretching vibration at 1282 nm. Meanwhile, there may be a significant amount of bound O-H in the manure gutter, such as polysaccharides, proteins, and other large molecular substances, which exhibit stretching vibrations at 1126 nm.

Temperature changes may affect the physical state and hydrogen bonding strength of these substances, thereby altering the near-infrared absorption characteristics and the position and intensity of absorption peaks. In contrast, the lagoon is at the end of the entire slurry treatment process, and a series of treatment processes in front of the lagoon are conducive to the decomposition of nitrogen-containing organic compounds such as amino acids and proteins, producing free N-H, which exhibits stretching vibration at 1470 nm. These functional groups may originate from different organic compounds or chemical environments, such as water molecules, alcohols, etc. In summary, the different microbial activities, chemical composition changes, physical state differences, temperature influence mechanisms, and concentration differences in both the manure gutter and lagoon ultimately lead to different performances of slurry samples in the temperature-sensitive band of near-infrared spectroscopy.

3.4.3 2D-COS Insights into Molecular Sequences and Model Optimization

By leveraging 2D-COS, we have identified a sequence of molecular changes triggered by temperature fluctuations, allowing for a more detailed understanding of spectral variability in dairy slurry systems. In addition, the findings of the 2D-COS analysis also offer new directions for optimizing the PLSR model as well. For the identified temperature-sensitive bands, special attention can be paid during feature selection by selectively weighting or excluding these regions, combined with algorithms such as piecewise direct standardization or adaptive PLSR, to reduce temperature sensitivity in future work [38]. For example, the two peaks at 1282 nm and 1126 nm in manure gutter samples, as well as the three peaks at 1470 nm, 1095 nm, and 969 nm in lagoon samples, mostly show negative absorption in the corrected spectra. However, some peaks that generate absorption peaks with high intensity in the corrected spectra do not show particular sensitivity to temperature changes. Temperature-insensitive spectral regions such as those highlighted in Fig. 4, could be selectively integrated into NIRS calibration models to build a model less susceptible to temperature noise. Secondly, the molecular response sequence (especially the preferential variation pattern of water related bands) reveals the inherent mechanism of temperature influence, based on which mechanism temperature correction terms can be

developed and integrated into the preprocessing steps or regression algorithms of PLSR. Furthermore, future machine learning models could incorporate 2D-COS-derived spectral data to enhance temperature correction algorithms, further improving NIRS measurement reliability in real-world conditions.

However, in the practical NIRS detection of dairy farm slurry, aside from temperature effects, it faces combined interference from various complex factors. Among these, fluctuations in suspended solids content, dynamic variations in moisture, and microbial activity constitute the primary interfering factors. Firstly, the suspended solids content exhibits significant spatiotemporal variation during slurry handling. Changes in particle size and composition cause spectral baseline drift and signal attenuation through light scattering effects, particularly affecting the on-site detection accuracy of portable devices. Secondly, the strong absorption peaks of slurry moisture may obscure the characteristic signals of other organic components, and their interaction with temperature further increases the spectral complexity. Furthermore, the microbial fermentation process from the manure gutter to the lagoon continuously alters the slurry's chemical composition, causing dynamic responses in specific spectral bands, which reflect the accumulation effects of microbial metabolites.

Based on the 2D-COS analytical framework, further resolution of multi-factor disturbances and model optimization can be achieved. On one hand, by designing orthogonal experiments involving temperature, suspended solids, and moisture content, 2D-COS can be utilized to quantify the contribution priority of each factor to the characteristic spectra. On the other hand, integrating the molecular response sequences identified by 2D-COS with Partial Least Squares Regression (PLSR) models allows for constructing dynamic correction algorithms to enhance monitoring accuracy. Ultimately, deploying portable NIRS devices at different process stages within the dairy farm (e.g., solid-liquid separation, fermentation stages) can validate the applicability of the 2D-COS correction model in practical scenarios, providing adaptive solutions for field detection.

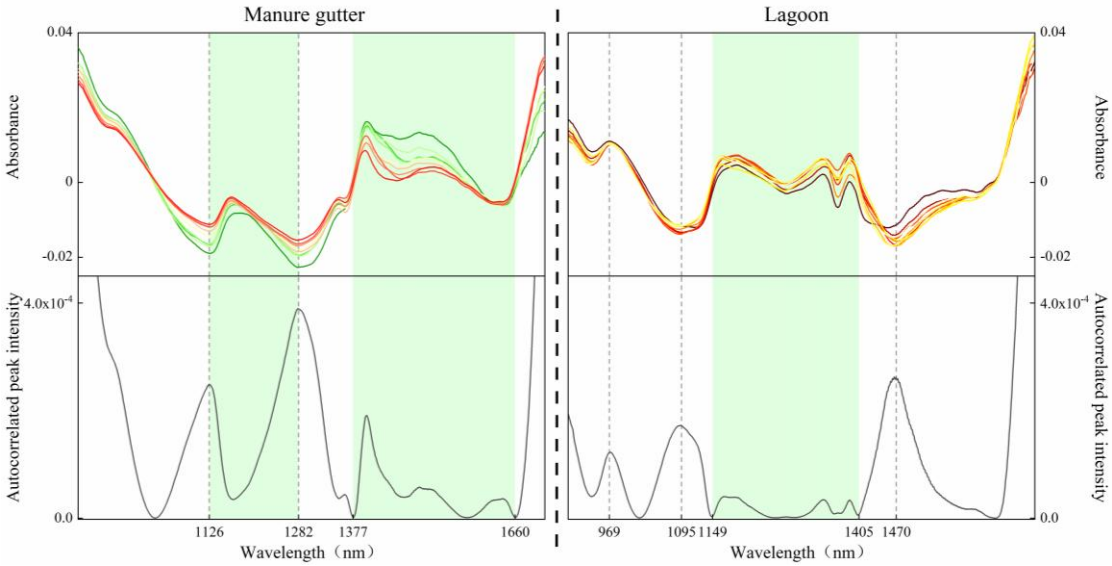


Fig. 4 Comparison of corrected spectra and autocorrelation spectra between the manure gutter and lagoon

4 Conclusion

This study applied PCA, spectral analysis, and 2D-COS analysis to investigate the temperature-dependent near-infrared spectral characteristics of dairy slurry samples. The research was conducted by collecting field samples and analyzing them using portable instruments, while simulating on-site environmental conditions to explore the mechanisms behind the challenges encountered during on-site inspections. Our results demonstrate the effectiveness of 2D-COS in identifying the sequence of functional group changes in mud under the influence of temperature. The findings highlight that temperature significantly influences the chemical composition of slurry, especially in the changes before and after anaerobic fermentation. As temperature increases, weaker hydrogen bonds break, leading to a decrease in absorbance peak intensity. Additionally, changes in associated and free O-H groups further confirm the influence of temperature on intermolecular forces. Through 2D-COS, we identified the interactions and sequential transformations of key functional groups, revealing that certain chemical bonds in the slurry are more susceptible to temperature-induced disruptions, affecting the stability of the entire system.

These insights could offerimportant implications for improving NIRS-based slurry analysis, particularly in the development of temperature correction models for real-time

monitoring and precision agriculture applications. The laboratory-based simulation of field conditions allowed for a controlled investigationof spectral interferences, thereby contributing tothe theoretical foundation for model optimization. By isolating temperature-induced spectral changes, this approach helps improve the accuracy of nutrient content prediction models. Accurate and real-time assessment of slurry composition is consideredcrucial for optimizing nutrient management strategies, as it can enablemore precise application of slurry as fertilizer, which may contribute tominimizing nutrient losses and optimizing resource utilization. Improved strategies could help farmers adjust application rates in response to real-time nutrient availability, reducing reliance on synthetic fertilizers and enhancing soil fertility while mitigating environmental risks such as nitrogen leaching and phosphorus runoff.

Additionally, the integration of 2D-COS-based temperature correction models in NIRS systems could facilitate the development of smart farm technologies that enable continuous monitoring of slurry characteristics. This would support automated nutrient management systems in precision agriculture, ensuring that slurry-derived nutrients are effectively recycled while reducing greenhouse gas emissions from inefficient slurry applications. Furthermore, these advancements contribute to regulatory compliance with environmental policies by providing farmers with accurate tools to meet nutrient management guidelines and improve overall sustainability in livestock farming.

Further research is needed to extend beyond temperature effects to explore other factors influencing manure spectral characteristics, such as turbidity, compositional heterogeneity, microbial activity, and storage conditions. The laboratory approach developed in this study—combining field sample collection with controlled experimentation—provides a framework for such investigations. A deeper microscopic analysis of manure spectra under varying conditions will lay the theoretical foundation for improving and optimizing rapid, non-destructive manure analysis techniques in practical applications, ensuring more efficient, data-driven, and environmentally responsible nutrient management strategies for dairy farming.

References

[1] Duan J.K., Liu H.B., Zhang X.M., Ren C.C., Wang C., Cheng L.X., Xu J.M., Gu B.J., Agricultural management practices in China enhance nitrogen sustainability and benefit human health, Nat. Food 5 (2024) 378-389.

[2] Wang P., Zhao R., Sun D., Li M.T., Mu M.R., Yang R.J., Zhang K.Q., Rapid quantitative analysis of nitrogen and phosphorus through the whole chain of manure management in dairy farms by fusion model, Spectrochimica Acta Part A: Molecular and Biomolecular Spectroscopy 249 (2021) 119300.

[3] Samadi, Sitti W.J., Agus A.M., Near infrared spectroscopy (NIRS) data analysis for a rapid and simultaneous prediction of feed nutritive parameters, Data in Brief 29 (2020) 105211.

[4] Li M.T., Sun D., Liu S.B., Zhang K.Q., Zhao R., Yang Z.J., Dynamic Prediction of Total N and P Contents in Slurry from Dairy Farms under Different Treatment Processes Using Near-Infrared Spectroscopy, Sustainability 16 (2024) 5083.

[5] Xu Y.M., Chen T.Y., Zhang H.X., Nuermaimaiti Y.N., Zhang S.Y., Wang F., Xiao J.X., Liu S., Shao W., Cao Z.J., Wang J.J., Chen Y., Application of Near-Infrared Reflectance Spectroscopy for Predicting Chemical Composition of Feces in Holstein Dairy Cows and Calves, ANIMALS 14 (2024).

[6] Kartal Z., Şahin O., Synthesis, spectroscopic, thermal, crystal structure properties and characterization of new Hofmann-type-like clathrates with 4-aminopyridine and water, Turkish Journal of Chemistry 45 (2021) 616-633.

[7] Morawietz T., Marsalek O., Pattenaude S.R., Streacker L.M., Ben A.D., Markland T.E., The interplay of structure and dynamics in the Raman spectrum of liquid water over the full frequency and temperature range, The Journal of Physical Chemistry Letters 9 (2018) 851-857.

[8] Li M.T., Sun D., Mu M.R., Liu H.X., Zhang K.Q., Yang R.J., Zhao R., Variation characteristics and rules of nitrogen and phosphorus contents throughout the slurry movement from scaled dairy farms in Tianjin, Transactions of the Chinese Society of Agricultural Engineering 36 (2020) 27-33.

[9] Sun D., Yang R.J., Li M.J., Mu M.R., Li M.T., Zhang K.Q., Zhao R., Influences of spring and autumn on the nitrogen and phosphorus contents of the slurry predicted by near-infrared spectrum model on dairy farms, Transactions of the Chinese Society of Agricultural Engineering 36 (2020) 197-205.

[10] Liang X.Y., Li X.Y., Lei T.W., Wang W., Gao Y., Study of sample temperature compensation in the measurement of soil moisture content, Measurement 44 (2011) 2200-2204.

[11] Wang T.Y., Tan Y., Chen Y.Z., Tan C.Y., Infrared spectral analysis for prediction of functional groups based on feature-aggregated deep learning, J. Chem. Inf. Model. 63 (2023) 4615-4622.

[12] Finzi A., Oberti R., Negri A.S., Perazzolo F., Cocolo G., Tambone F., Cabassi G., Provolo G., Effects of measurement technique and sample preparation on NIR spectroscopy analysis of livestock slurry and digestates, Biosyst. Eng. 134 (2015) 42-54.

[13] Talebanpour B.E., Akhond M., Hemmateenejad B., Mid-infrared spectroscopy study of aqueous solution of ethylene glycol using chemometrics analysis and two‐dimensional correlation spectroscopy. Journal of Chemometrics, 37 (2023).

[14] Park Y., Jin S., Noda I., Jung Y.M., Continuing progress in the field of two-dimensional correlation spectroscopy (2D-COS), part I. Yesterday and today. Spectrochimica Acta Part A: Molecular and Biomolecular Spectroscopy, 281 (2022), 121573.

[15] Gui X., Liu C., Li F., Wang J., Effect of pyrolysis temperature on the composition of DOM in manure-derived biochar, Ecotoxicology and Environmental Safety. 197 (2020) 110597.
[16] Huang Y., Tian Y., Xie L., Liu Y., Dai B., Guo X., Yang Y., The application of two-dimensional correlation spectroscopy for the binding properties of heavy metals onto digestate-derived DOM from anaerobic digestion of chicken manure, Ecotoxicology and Environmental Safety. 204 (2020) 111129.
[17] Liu L.Y., Yang R.J., Zhang J., Gong G.M., Yang Y.R., Recent progress in two-dimensional correlation spectroscopy for the environmental detection and analysis, J. Mol. Struct. 1214 (2020) 128263.
[18] Zhang C., Wang W., Pan Y., Cheng L., Zhai S., Gao X., A two-stage method for real-time baseline drift compensation in gas sensors, Measurement Sci. Technol. 33 (2022) 045108.
[19] Kiran H., Ali A., Rodgers T., Mendoza C., Baker M., Martin P., Evaluation of temperature compensation methods for a near‐infrared calibration to predict the viscosity of micellar liquids. Journal of Chemometrics, 34 (2020).
[20] Bruno T.J., Svoronos P.D.N., CRC Handbook of Fundamental Spectroscopic Correlation Charts. 2005.
[21] Workman Jr.J., Weyer L., Practical Guide and Spectral Atlas for Interpretive Near-Infrared Spectroscopy (2nd ed.). CRC Press. 2012.
[22] Wang S.Q., Kong D.W., Zhang K.Q., Chang X.P., Lu Z.W., Du L.Z., Effectiveness of layered inoculation in solid-state anaerobic co-digestion of pig manure and corn straw: Focus on macro-, micro-, and genetic-levels. Bioresource Technology, 355 (2022).
[23] Ma J.Y., Mitigating transformation of ammonia and fatty acids during anaerobic digestion by biochar coupled iron nanoparticles, Doctoral dissertation, Northwest A&F University (2021).
[24] Li D.N., Zhang K.Q., Kong D.W., Liang J.F., Du L.Z., Effects of non-mixed seeding on methane production characteristics of the batch dry anaerobic digestion of pig manure, Chinese Journal of Environmental Engineering, 15 (2021) 279-288.
[25] Fuchs W., Wang X.M., Gabauer W., Ortner M., Li Z.F., Tackling ammonia inhibition for efficient biogas production from chicken manure: Status and technical trends in Europe and China, Renew. Sustain. Energy Rev. 97 (2018) 186-199.
[26] Kassayová M., Jiménez-Redondo M., Sarka J., Dohnal P., Glosík J., Caselli P., Jusko P., Rovibrational overtone and combination bands of the HCNH＋ ion, Spectrochimica Acta Part A: Molecular and Biomolecular Spectroscopy, 337 (2025) 126040.
[27] You Z.H., Zhuo L.L., Yang X.L., Hong H.M., Liu Z.H., Gong Z.Y., Cheng F., Food Research Applications of Two-Dimensional Correlation Spectroscopy. Applied Spectroscopy Reviews, 50 (2015), 840-858.
[28] Noda I., Ozaki Y., Two-dimensional correlation spectroscopy - Applications in vibrational and optical spectroscopy, John Wiley & Sons, Ltd (2004).
[29] Ouyang S.L., Li Z.Q., Wu N.N., Li Z.W., Sun C.L., Fan L.M., Temperature effect on the hydrogen bonding behavior between DMSO and water in aqueous DMSO solutions studied by raman spectroscopy. Guang Pu Xue Yu Guang Pu Fen Xi, 33(2013), 2425-2428.
[30] Bromberg S.E., Yang H., Asplund M.C., Lian T., McNamara B.K., Kotz K.T., Yeston J.S., Wilkens M., Frei H., Bergman R.G., Harris C.B., The mechanism of a C-H bond activation reaction in room-temperature alkane solution, Science (1997).

650 [31] Watanabe A., Morita S., Ozaki Y., Study on temperature-dependent changes in hydrogen bonds
651 in cellulose Iβ by infrared spectroscopy with perturbation-correlation moving-window two-
652 dimensional correlation spectroscopy. Biomacromolecules, 7 (2006) 3164-3170.
653 [32] Patrinoiu G., Musuc A. M., Calderon-Moreno J. M., Florea M., Neatu F., Ionita P, Honey-
654 Derived Hydrochar Containing 2,2,6,6-tetramethylpiperidine-1-oxyl Free Radical for Degradation
655 of Aqueous Organic Pollutants. Environmental Processes, 11 (2024).
656 [33] Aloui F., Lecamp L., Lebaudy P., Burel F., Relationships between refractive index change and
657 light scattering during photopolymerization of acrylic composite formulations, J. Eur. Ceram. Soc.
658 36 (2016) 1805-1809.
659 [34] Xu J.L., Dorrepaal R.M., Martinez-Gonzalez J., Tsenkova R., Gowen A.A., Near-infrared
660 multivariate model transfer for quantification of different hydrogen bonding species in aqueous
661 systems. Journal of Chemometrics, 34(2020), e3274.
662 [35] Tan J.H., Sun Y., Ma L., Feng H.Y., Guo Y.C., Cai W.S., Shao X.G., Knowledge-based genetic
663 algorithm for resolving the near-infrared spectrum and understanding the water structures in
664 aqueous solution. Chemometrics and Intelligent Laboratory Systems, 206(2020), 104150.
665 [36] Kondo A., Kurosawa R., Ryu J., Matsuoka M., Takeuchi M., Investigation on the mechanisms
666 of Mg (OH) 2 dehydration and MgO hydration by near-infrared spectroscopy. The Journal of
667 Physical Chemistry C, 125(2021), 10937-10947.
668 [37] Muratova M.E., Mikheev I.V., Volkov D.S., Proskurnin M.A., Application of two-dimensional
669 correlation spectroscopy to chemical analysis, Journal of Analytical Chemistry, 79 (2024) 339-365.
670 [38] Díaz Olivares J.A., Grauwels S., Fu X.Y., Adriaens I., Saeys W., Bendoula R., Roger J.M.,
671 Aernouts B., Temperature Correction of Near-Infrared Spectra of Raw Milk, Chemometrics and
672 Intelligent Laboratory Systems, 255 (2024) 105251.